Fermilab-Pub-08/062-E

Measurement of the ratio of the $p\bar{p} \to W+c$-jet cross section to the inclusive $p\bar{p} \to W+$jets cross section

V.M. Abazov[36], B. Abbott[75], M. Abolins[65], B.S. Acharya[29], M. Adams[51], T. Adams[49], E. Aguilo[6], S.H. Ahn[31], M. Ahsan[59], G.D. Alexeev[36], G. Alkhazov[40], A. Alton[64,a], G. Alverson[63], G.A. Alves[2], M. Anastasoaie[35], L.S. Ancu[35], T. Andeen[53], S. Anderson[45], B. Andrieu[17], M.S. Anzelc[53], M. Aoki[50], Y. Arnoud[14], M. Arov[60], M. Arthaud[18], A. Askew[49], B. Åsman[41], A.C.S. Assis Jesus[3], O. Atramentov[49], C. Avila[8], C. Ay[24], F. Badaud[13], A. Baden[61], L. Bagby[50], B. Baldin[50], D.V. Bandurin[59], P. Banerjee[29], S. Banerjee[29], E. Barberis[63], A.-F. Barfuss[15], P. Bargassa[80], P. Baringer[58], J. Barreto[2], J.F. Bartlett[50], U. Bassler[18], D. Bauer[43], S. Beale[6], A. Bean[58], M. Begalli[3], M. Begel[73], C. Belanger-Champagne[41], L. Bellantoni[50], A. Bellavance[50], J.A. Benitez[65], S.B. Beri[27], G. Bernardi[17], R. Bernhard[23], I. Bertram[42], M. Besançon[18], R. Beuselinck[43], V.A. Bezzubov[39], P.C. Bhat[50], V. Bhatnagar[27], C. Biscarat[20], G. Blazey[52], F. Blekman[43], S. Blessing[49], D. Bloch[19], K. Bloom[67], A. Boehnlein[50], D. Boline[62], T.A. Bolton[59], G. Borissov[42], T. Bose[77], A. Brandt[78], R. Brock[65], G. Brooijmans[70], A. Bross[50], D. Brown[81], N.J. Buchanan[49], D. Buchholz[53], M. Buehler[81], V. Buescher[22], V. Bunichev[38], S. Burdin[42,b], S. Burke[45], T.H. Burnett[82], C.P. Buszello[43], J.M. Butler[62], P. Calfayan[25], S. Calvet[16], J. Cammin[71], W. Carvalho[3], B.C.K. Casey[50], H. Castilla-Valdez[33], S. Chakrabarti[18], D. Chakraborty[52], K. Chan[6], K.M. Chan[55], A. Chandra[48], F. Charles[19,‡], E. Cheu[45], F. Chevallier[14], D.K. Cho[62], S. Choi[32], B. Choudhary[28], L. Christofek[77], T. Christoudias[43], S. Cihangir[50], D. Claes[67], Y. Coadou[6], M. Cooke[80], W.E. Cooper[50], M. Corcoran[80], F. Couderc[18], M.-C. Cousinou[15], S. Crépé-Renaudin[14], D. Cutts[77], M. Ćwiok[30], H. da Motta[2], A. Das[45], G. Davies[43], K. De[78], S.J. de Jong[35], E. De La Cruz-Burelo[64], C. De Oliveira Martins[3], J.D. Degenhardt[64], F. Déliot[18], M. Demarteau[50], R. Demina[71], D. Denisov[50], S.P. Denisov[39], S. Desai[50], H.T. Diehl[50], M. Diesburg[50], A. Dominguez[67], H. Dong[72], L.V. Dudko[38], L. Duflot[16], S.R. Dugad[29], D. Duggan[49], A. Duperrin[15], J. Dyer[65], A. Dyshkant[52], M. Eads[67], D. Edmunds[65], J. Ellison[48], V.D. Elvira[50], Y. Enari[77], S. Eno[61], P. Ermolov[38], H. Evans[54], A. Evdokimov[73], V.N. Evdokimov[39], A.V. Ferapontov[59], T. Ferbel[71], F. Fiedler[24], F. Filthaut[35], W. Fisher[50], H.E. Fisk[50], M. Fortner[52], H. Fox[42], S. Fu[50], S. Fuess[50], T. Gadfort[70], C.F. Galea[35], E. Gallas[50], C. Garcia[71], A. Garcia-Bellido[82], V. Gavrilov[37], P. Gay[13], W. Geist[19], D. Gelé[19], C.E. Gerber[51], Y. Gershtein[49], D. Gillberg[6], G. Ginther[71], N. Gollub[41], B. Gómez[8], A. Goussiou[82], P.D. Grannis[72], H. Greenlee[50], Z.D. Greenwood[60], E.M. Gregores[4], G. Grenier[20], Ph. Gris[13], J.-F. Grivaz[16], A. Grohsjean[25], S. Grünendahl[50], M.W. Grünewald[30], F. Guo[72], J. Guo[72], G. Gutierrez[50], P. Gutierrez[75], A. Haas[70], N.J. Hadley[61], P. Haefner[25], S. Hagopian[49], J. Haley[68], I. Hall[65], R.E. Hall[47], L. Han[7], K. Harder[44], A. Harel[71], R. Harrington[63], J.M. Hauptman[57], R. Hauser[65], J. Hays[43], T. Hebbeker[21], D. Hedin[52], J.G. Hegeman[34], J.M. Heinmiller[51], A.P. Heinson[48], U. Heintz[62], C. Hensel[58], K. Herner[72], G. Hesketh[63], M.D. Hildreth[55], R. Hirosky[81], J.D. Hobbs[72], B. Hoeneisen[12], H. Hoeth[26], M. Hohlfeld[22], S.J. Hong[31], S. Hossain[75], P. Houben[34], Y. Hu[72], Z. Hubacek[10], V. Hynek[9], I. Iashvili[69], R. Illingworth[50], A.S. Ito[50], S. Jabeen[62], M. Jaffré[16], S. Jain[75], K. Jakobs[23], C. Jarvis[61], R. Jesik[43], K. Johns[45], C. Johnson[70], M. Johnson[50], A. Jonckheere[50], P. Jonsson[43], A. Juste[50], E. Kajfasz[15], A.M. Kalinin[36], J.M. Kalk[60], S. Kappler[21], D. Karmanov[38], P.A. Kasper[50], I. Katsanos[70], D. Kau[49], V. Kaushik[78], R. Kehoe[79], S. Kermiche[15], N. Khalatyan[50], A. Khanov[76], A. Kharchilava[69], Y.M. Kharzheev[36], D. Khatidze[70], T.J. Kim[31], M.H. Kirby[53], M. Kirsch[21], B. Klima[50], J.M. Kohli[27], J.-P. Konrath[23], V.M. Korablev[39], A.V. Kozelov[39], J. Kraus[65], D. Krop[54], T. Kuhl[24], A. Kumar[69], A. Kupco[11], T. Kurča[20], J. Kvita[9], F. Lacroix[13], D. Lam[55], S. Lammers[70], G. Landsberg[77], P. Lebrun[20], W.M. Lee[50], A. Leflat[38], J. Lellouch[17], J. Leveque[45], J. Li[78], L. Li[48], Q.Z. Li[50], S.M. Lietti[5], J.G.R. Lima[52], D. Lincoln[50], J. Linnemann[65], V.V. Lipaev[39], R. Lipton[50], Y. Liu[7], Z. Liu[6], A. Lobodenko[40], M. Lokajicek[11], P. Love[42], H.J. Lubatti[82], R. Luna[3], A.L. Lyon[50], A.K.A. Maciel[2], D. Mackin[80], R.J. Madaras[46], P. Mättig[26], C. Magass[21], A. Magerkurth[64], P.K. Mal[82], H.B. Malbouisson[3], S. Malik[67], V.L. Malyshev[36], H.S. Mao[50], Y. Maravin[59], B. Martin[14], R. McCarthy[72], A. Melnitchouk[66], L. Mendoza[8], P.G. Mercadante[5], M. Merkin[38], K.W. Merritt[50], A. Meyer[21], J. Meyer[22,d], T. Millet[20], J. Mitrevski[70], J. Molina[3], R.K. Mommsen[44], N.K. Mondal[29], R.W. Moore[6], T. Moulik[58], G.S. Muanza[20], M. Mulders[50], M. Mulhearn[70], O. Mundal[22], L. Mundim[3], E. Nagy[15], M. Naimuddin[50], M. Narain[77], N.A. Naumann[35], H.A. Neal[64], J.P. Negret[8], P. Neustroev[40], H. Nilsen[23], H. Nogima[3], S.F. Novaes[5], T. Nunnemann[25], V. O'Dell[50], D.C. O'Neil[6], G. Obrant[40], C. Ochando[16], D. Onoprienko[59], N. Oshima[50], N. Osman[43], J. Osta[55], R. Otec[10], G.J. Otero y Garzón[50], M. Owen[44], P. Padley[80], M. Pangilinan[77], N. Parashar[56], S.-J. Park[71], S.K. Park[31],

J. Parsons[70], R. Partridge[77], N. Parua[54], A. Patwa[73], G. Pawloski[80], B. Penning[23], M. Perfilov[38], K. Peters[44], Y. Peters[26], P. Pétroff[16], M. Petteni[43], R. Piegaia[1], J. Piper[65], M.-A. Pleier[22], P.L.M. Podesta-Lerma[33,c], V.M. Podstavkov[50], Y. Pogorelov[55], M.-E. Pol[2], P. Polozov[37], B.G. Pope[65], A.V. Popov[39], C. Potter[6], W.L. Prado da Silva[3], H.B. Prosper[49], S. Protopopescu[73], J. Qian[64], A. Quadt[22,d], B. Quinn[66], A. Rakitine[42], M.S. Rangel[2], K. Ranjan[28], P.N. Ratoff[42], P. Renkel[79], S. Reucroft[63], P. Rich[44], J. Rieger[54], M. Rijssenbeek[72], I. Ripp-Baudot[19], F. Rizatdinova[76], S. Robinson[43], R.F. Rodrigues[3], M. Rominsky[75], C. Royon[18], P. Rubinov[50], R. Ruchti[55], G. Safronov[37], G. Sajot[14], A. Sánchez-Hernández[33], M.P. Sanders[17], A. Santoro[3], G. Savage[50], L. Sawyer[60], T. Scanlon[43], D. Schaile[25], R.D. Schamberger[72], Y. Scheglov[40], H. Schellman[53], T. Schliephake[26], C. Schwanenberger[44], A. Schwartzman[68], R. Schwienhorst[65], J. Sekaric[49], H. Severini[75], E. Shabalina[51], M. Shamim[59], V. Shary[18], A.A. Shchukin[39], R.K. Shivpuri[28], V. Siccardi[19], V. Simak[10], V. Sirotenko[50], P. Skubic[75], P. Slattery[71], D. Smirnov[55], G.R. Snow[67], J. Snow[74], S. Snyder[73], S. Söldner-Rembold[44], L. Sonnenschein[17], A. Sopczak[42], M. Sosebee[78], K. Soustruznik[9], B. Spurlock[78], J. Stark[14], J. Steele[60], V. Stolin[37], D.A. Stoyanova[39], J. Strandberg[64], S. Strandberg[41], M.A. Strang[69], E. Strauss[72], M. Strauss[75], R. Ströhmer[25], D. Strom[53], L. Stutte[50], S. Sumowidagdo[49], P. Svoisky[55], A. Sznajder[3], P. Tamburello[45], A. Tanasijczuk[1], W. Taylor[6], J. Temple[45], B. Tiller[25], F. Tissandier[13], M. Titov[18], V.V. Tokmenin[36], T. Toole[61], I. Torchiani[23], T. Trefzger[24], D. Tsybychev[72], B. Tuchming[18], C. Tully[68], P.M. Tuts[70], R. Unalan[65], L. Uvarov[40], S. Uvarov[40], S. Uzunyan[52], B. Vachon[6], P.J. van den Berg[34], R. Van Kooten[54], W.M. van Leeuwen[34], N. Varelas[51], E.W. Varnes[45], I.A. Vasilyev[39], M. Vaupel[26], P. Verdier[20], L.S. Vertogradov[36], M. Verzocchi[50], F. Villeneuve-Seguier[43], P. Vint[43], P. Vokac[10], E. Von Toerne[59], M. Voutilainen[68,e], R. Wagner[68], H.D. Wahl[49], L. Wang[61], M.H.L.S. Wang[50], J. Warchol[55], G. Watts[82], M. Wayne[55], G. Weber[24], M. Weber[50], L. Welty-Rieger[54], A. Wenger[23,f], N. Wermes[22], M. Wetstein[61], A. White[78], D. Wicke[26], G.W. Wilson[58], S.J. Wimpenny[48], M. Wobisch[60], D.R. Wood[63], T.R. Wyatt[44], Y. Xie[77], S. Yacoob[53], R. Yamada[50], M. Yan[61], T. Yasuda[50], Y.A. Yatsunenko[36], K. Yip[73], H.D. Yoo[77], S.W. Youn[53], J. Yu[78], A. Zatserklyaniy[52], C. Zeitnitz[26], T. Zhao[82], B. Zhou[64], J. Zhu[72], M. Zielinski[71], D. Zieminska[54], A. Zieminski[54,‡], L. Zivkovic[70], V. Zutshi[52], and E.G. Zverev[38]

(The DØ Collaboration)

[1]*Universidad de Buenos Aires, Buenos Aires, Argentina*
[2]*LAFEX, Centro Brasileiro de Pesquisas Físicas, Rio de Janeiro, Brazil*
[3]*Universidade do Estado do Rio de Janeiro, Rio de Janeiro, Brazil*
[4]*Universidade Federal do ABC, Santo André, Brazil*
[5]*Instituto de Física Teórica, Universidade Estadual Paulista, São Paulo, Brazil*
[6]*University of Alberta, Edmonton, Alberta, Canada, Simon Fraser University, Burnaby, British Columbia, Canada, York University, Toronto, Ontario, Canada, and McGill University, Montreal, Quebec, Canada*
[7]*University of Science and Technology of China, Hefei, People's Republic of China*
[8]*Universidad de los Andes, Bogotá, Colombia*
[9]*Center for Particle Physics, Charles University, Prague, Czech Republic*
[10]*Czech Technical University, Prague, Czech Republic*
[11]*Center for Particle Physics, Institute of Physics, Academy of Sciences of the Czech Republic, Prague, Czech Republic*
[12]*Universidad San Francisco de Quito, Quito, Ecuador*
[13]*LPC, Univ Blaise Pascal, CNRS/IN2P3, Clermont, France*
[14]*LPSC, Université Joseph Fourier Grenoble 1, CNRS/IN2P3, Institut National Polytechnique de Grenoble, France*
[15]*CPPM, IN2P3/CNRS, Université de la Méditerranée, Marseille, France*
[16]*LAL, Univ Paris-Sud, IN2P3/CNRS, Orsay, France*
[17]*LPNHE, IN2P3/CNRS, Universités Paris VI and VII, Paris, France*
[18]*DAPNIA/Service de Physique des Particules, CEA, Saclay, France*
[19]*IPHC, Université Louis Pasteur et Université de Haute Alsace, CNRS/IN2P3, Strasbourg, France*
[20]*IPNL, Université Lyon 1, CNRS/IN2P3, Villeurbanne, France and Université de Lyon, Lyon, France*
[21]*III. Physikalisches Institut A, RWTH Aachen, Aachen, Germany*
[22]*Physikalisches Institut, Universität Bonn, Bonn, Germany*
[23]*Physikalisches Institut, Universität Freiburg, Freiburg, Germany*
[24]*Institut für Physik, Universität Mainz, Mainz, Germany*
[25]*Ludwig-Maximilians-Universität München, München, Germany*
[26]*Fachbereich Physik, University of Wuppertal, Wuppertal, Germany*
[27]*Panjab University, Chandigarh, India*

[28]*Delhi University, Delhi, India*
[29]*Tata Institute of Fundamental Research, Mumbai, India*
[30]*University College Dublin, Dublin, Ireland*
[31]*Korea Detector Laboratory, Korea University, Seoul, Korea*
[32]*SungKyunKwan University, Suwon, Korea*
[33]*CINVESTAV, Mexico City, Mexico*
[34]*FOM-Institute NIKHEF and University of Amsterdam/NIKHEF, Amsterdam, The Netherlands*
[35]*Radboud University Nijmegen/NIKHEF, Nijmegen, The Netherlands*
[36]*Joint Institute for Nuclear Research, Dubna, Russia*
[37]*Institute for Theoretical and Experimental Physics, Moscow, Russia*
[38]*Moscow State University, Moscow, Russia*
[39]*Institute for High Energy Physics, Protvino, Russia*
[40]*Petersburg Nuclear Physics Institute, St. Petersburg, Russia*
[41]*Lund University, Lund, Sweden, Royal Institute of Technology and Stockholm University, Stockholm, Sweden, and Uppsala University, Uppsala, Sweden*
[42]*Lancaster University, Lancaster, United Kingdom*
[43]*Imperial College, London, United Kingdom*
[44]*University of Manchester, Manchester, United Kingdom*
[45]*University of Arizona, Tucson, Arizona 85721, USA*
[46]*Lawrence Berkeley National Laboratory and University of California, Berkeley, California 94720, USA*
[47]*California State University, Fresno, California 93740, USA*
[48]*University of California, Riverside, California 92521, USA*
[49]*Florida State University, Tallahassee, Florida 32306, USA*
[50]*Fermi National Accelerator Laboratory, Batavia, Illinois 60510, USA*
[51]*University of Illinois at Chicago, Chicago, Illinois 60607, USA*
[52]*Northern Illinois University, DeKalb, Illinois 60115, USA*
[53]*Northwestern University, Evanston, Illinois 60208, USA*
[54]*Indiana University, Bloomington, Indiana 47405, USA*
[55]*University of Notre Dame, Notre Dame, Indiana 46556, USA*
[56]*Purdue University Calumet, Hammond, Indiana 46323, USA*
[57]*Iowa State University, Ames, Iowa 50011, USA*
[58]*University of Kansas, Lawrence, Kansas 66045, USA*
[59]*Kansas State University, Manhattan, Kansas 66506, USA*
[60]*Louisiana Tech University, Ruston, Louisiana 71272, USA*
[61]*University of Maryland, College Park, Maryland 20742, USA*
[62]*Boston University, Boston, Massachusetts 02215, USA*
[63]*Northeastern University, Boston, Massachusetts 02115, USA*
[64]*University of Michigan, Ann Arbor, Michigan 48109, USA*
[65]*Michigan State University, East Lansing, Michigan 48824, USA*
[66]*University of Mississippi, University, Mississippi 38677, USA*
[67]*University of Nebraska, Lincoln, Nebraska 68588, USA*
[68]*Princeton University, Princeton, New Jersey 08544, USA*
[69]*State University of New York, Buffalo, New York 14260, USA*
[70]*Columbia University, New York, New York 10027, USA*
[71]*University of Rochester, Rochester, New York 14627, USA*
[72]*State University of New York, Stony Brook, New York 11794, USA*
[73]*Brookhaven National Laboratory, Upton, New York 11973, USA*
[74]*Langston University, Langston, Oklahoma 73050, USA*
[75]*University of Oklahoma, Norman, Oklahoma 73019, USA*
[76]*Oklahoma State University, Stillwater, Oklahoma 74078, USA*
[77]*Brown University, Providence, Rhode Island 02912, USA*
[78]*University of Texas, Arlington, Texas 76019, USA*
[79]*Southern Methodist University, Dallas, Texas 75275, USA*
[80]*Rice University, Houston, Texas 77005, USA*
[81]*University of Virginia, Charlottesville, Virginia 22901, USA and*
[82]*University of Washington, Seattle, Washington 98195, USA*

(Dated: March 14, 2008)

We present a measurement of the fraction of inclusive W+jets events produced with net charm quantum number ± 1, denoted W+c-jet, in $p\bar{p}$ collisions at $\sqrt{s} = 1.96$ TeV using approximately 1 fb^{-1} of data collected by the D0 detector at the Fermilab Tevatron Collider. We identify the W+jets events via the leptonic W boson decays. Candidate W+c-jet events are selected by requiring a jet containing a muon in association with a reconstructed W boson and exploiting the charge correlation between this muon and W boson decay lepton to perform a nearly model-independent background subtraction. We measure the fraction of W+c-jet events in the inclusive W+jets sample for jet $p_T > 20$ GeV and pseudorapidity $|\eta| < 2.5$ to be $0.074 \pm 0.019(\text{stat.})\pm^{0.012}_{0.014}(\text{syst.})$, in agreement with theoretical predictions. The probability that background fluctuations could produce the observed fraction of W+c-jet events is estimated to be 2.5×10^{-4}, which corresponds to a 3.5 σ statistical significance.

PACS numbers: 12.15.Ji, 12.38.Qk, 13.85.Ni, 13.85.Qk, 14.70.Fm, 14.65.Dw

In hadron-hadron collisions, the W/Z+b- or c-jet final state can signal the presence of new physics; however, only a few measurements [1, 2, 3] of cross sections for these standard model processes exist. Charm quark production in association with a W boson can be a significant background, for example, to top quark pair, single top quark and Higgs boson productions, and to supersymmetric top quark (stop) pair production when only the $\tilde{t} \to c\tilde{\chi}^0_1$ decay channel is allowed by the mass difference between the stop quark and the neutralino. Moreover, as the squared Cabibbo-Kobayashi-Maskawa matrix element, $|V_{cd}|^2$, suppresses the expected leading order d quark-gluon fusion production mechanism, W+c-quark production provides direct sensitivity to the proton's s quark parton distribution function (PDF), $s(x, Q^2)$, where x is the momentum fraction of the proton carried by the s-quark and $\sqrt{Q^2}$ is the hard scatter scale [4]. This PDF has been measured directly only in fixed target neutrino-nucleon deep inelastic scattering experiments using relatively low momentum transfer squared, Q^2, of the order $1 - 100$ GeV^2 [5, 6, 7, 8, 9, 10, 11]. A probe of the s quark PDF at the Tevatron tests the universality of $s(x, Q^2)$ and its QCD evolution up to $Q^2 = 10^4$ GeV^2. The strange quark PDF initiates both standard model (e.g., $sg \to W^- + c$) and possible new physics processes (e.g., $s\bar{c} \to H^-$) [12] at both the Fermilab Tevatron and CERN LHC colliders.

In this Letter, we present a measurement of the cross section ratio $\sigma(p\bar{p} \to W+c\text{-jet})\ /\sigma(p\bar{p} \to W+\text{jets})$ as a function of jet transverse momentum p_T, where W+c-jet denotes a W boson plus jets final state in which the jets have a net charm quantum number $C = \pm 1$, and W+jets denotes any W boson final state with at least one jet. Several experimental uncertainties (e.g., luminosity, jet energy scale, and reconstruction efficiency) and theoretical uncertainties (e.g., renormalization and factorization scales) largely cancel in this ratio.

This measurement utilizes approximately 1 fb^{-1} of $p\bar{p}$ collision data at a center-of-mass energy $\sqrt{s} = 1.96$ TeV collected with the D0 detector at the Fermilab Tevatron collider. We identify W bosons through their leptonic decays, $W \to \ell\nu$, where $\ell = e, \mu$. W bosons decaying to tau leptons are included for leptonic tau decays $\tau \to e\bar{\nu}_e\nu_\tau$ or $\tau \to \mu\bar{\nu}_\mu\nu_\tau$. The electron or muon from W boson decays are required to be isolated, and their transverse momentum p_T must satisfy $p_T > 20$ GeV. The presence of a neutrino is inferred from the requirement that the missing transverse energy $\not\!\!E_T$ satisfies $\not\!\!E_T > 20$ GeV. Jets are defined using the iterative seed-based midpoint cone algorithm [13] with cone radius of 0.5. We restrict the transverse momentum of the jet to $p_T > 20$ GeV after it is calibrated for the calorimeter jet energy scale (JES), and its pseudorapidity to $|\eta| < 2.5$, where $\eta = -\ln[\tan(\theta/2)]$ and θ is the polar angle with respect to the proton beam direction. We correct the jet measurement to the particle level [14] for comparison with theory.

A muon reconstructed within a jet (a "jet-muon") identifies that jet (a "μ-tagged jet") as a charm quark candidate. Events containing a jet-muon enrich a sample in b/c semileptonic decays. Events with the jet-muon's charge opposite to or equal to that of the W boson are denoted as "OS" or "SS" events, respectively. In the W+c-jet process, the charm quark decays into a muon carrying an opposite-sign charge compared to that carried by the W boson, and the numbers of OS and SS events, N_{OS} and N_{SS}, respectively, satisfy $N_{\text{OS}} \gg N_{\text{SS}}$. In the W+c-jet sample, N_{SS} can be non-zero because a jet initiated by a c quark has a small probability of containing a muon from the decay of particles other than the leading charm quark. Other vector boson+jets physics processes (W+g, W+$c\bar{c}$, W+$b\bar{b}$, Z+jets) can produce μ-tagged jets, but the charge of the jet-muon is uncorrelated with that of the boson, hence $N_{\text{OS}} \approx N_{\text{SS}}$ for these sources. Processes with light-quark (u, d or s) initiated jets recoiling against the W boson can produce a small fraction of charge-correlated μ-tagged jets owing to leading particle effects [15]. Background from WW production contributes only a small amount to the signal sample. The WZ and ZZ processes only rarely produce charge-correlated jets. Other final states that can produce charge-correlated jets ($t\bar{t}$, $t\bar{b}$, W+$b\bar{c}$ and W+b) are suppressed by small production cross sections or tiny CKM matrix elements. These considerations allow a measurement of the W+c-jet production rate from OS events with the backgrounds determined *in situ* from SS events, up to small weakly model-dependent theory corrections.

The D0 detector [16] is a multi-purpose device built to investigate $p\bar{p}$ collisions. The innermost silicon microstrip detectors followed by the scintillating fiber tracking detector, covering pseudorapidity $|\eta| \lesssim 3.0$ and located inside the 2 T superconducting solenoid, are used for tracking and vertexing. The liquid-argon and uranium calorimeter, a finely segmented detector in the transverse and the longitudinal directions, is used as the primary tool to reconstruct electrons, jets, and the missing transverse energy. It is housed in three cryostats, one central calorimeter in the region $|\eta| < 1.1$ and two end caps extending the coverage to $|\eta| \approx 4.0$. The outermost subsystem of the D0 detector is the muon spectrometer, consisting of three layers of muon tracking subdetectors and scintillation trigger counters, which is used to construct muons up to $|\eta| \approx 2.0$. The first layer is situated before the 1.8 T iron toroid and the other two layers are outside, enclosing the detector.

Candidate events in the electron (muon) decay channel of the W boson must pass at least one of the single electron (muon) three-level (L1, L2 and L3) triggers used in each data taking period. Each level of trigger imposes tighter restrictions on the events compared to those of the preceding level. The single muon triggers at L1 impose hit requirements in the muon scintillators. Some of the triggers also require spatially matched hits in the muon tracking detectors. The conditions at L2 require a reconstructed muon with p_T above a threshold in the range 0 – 5 GeV for various triggers. At L3, certain triggers require a track reconstructed in the inner tracking system with $p_T > 10$ GeV. The ratio measurement benefits from full cancellation of the trigger efficiency in the electron channel. This cancellation is partial in the muon channel due to the presence of two muons in the W+c-jet sample.

Selection of $W \to e\nu$ candidates begins with the requirement that a cluster of energy be found that is consistent with the presence of an electron in the calorimeter. The cluster must: have at least 90% of its energy contained in the electromagnetic part of the calorimeter; have a reconstructed track from the inner tracking system pointing to it; be isolated from other clusters in that the fraction of the energy deposited in an annulus ($0.2 < \Delta\mathcal{R} = \sqrt{(\Delta\phi)^2 + (\Delta\eta)^2} < 0.4$, where ϕ is the azimuthal angle) around the EM cluster is less than 15% of the electromagnetic energy within the cone of radius $\Delta\mathcal{R} = 0.2$; have longitudinal and transverse energy deposition profiles consistent with those expected for an electron; and satisfy a likelihood discriminant selection that combines tracker and calorimeter information using the expected distributions for electrons and jet background. The electron track's point of closest approach to the z-axis must be within 3 cm of the $p\bar{p}$ interaction point, which must lie within 60 cm of the nominal detector center.

Selection of $W \to \mu\nu$ candidates begins by requiring that a muon candidate be found in the muon spectrometer with a track matched to one found in the central tracker. Rejection of cosmic ray background events demands that the central tracker track pass within 0.02 or 0.2 cm of the beam crossing point in the transverse plane, depending on whether the track is reconstructed with or without hits, respectively, in the silicon detector, and that the point of closest approach of the track should be within 3 cm of the interaction point along the z-axis. Further cosmic ray rejection comes from scintillator timing information in the muon spectrometer. Requiring the W boson candidate muon track to be separated from the axis formed by any jet found in the event by $\Delta\mathcal{R}(\mu, \text{jet}) > 0.5$ suppresses backgrounds from semileptonic decays of heavy flavor quarks in multi-jet events.

For the final selection in both channels, each event must satisfy the transverse mass requirement $40 \leq M_T \leq 120$ GeV, where $M_T = \sqrt{2\not\!\!E_T p_T^\ell \left[1 - \cos\Delta\phi(\not\!\!E_T, p_T^\ell)\right]}$ is computed from the isolated lepton p_T^ℓ and the $\not\!\!E_T$, have an azimuthal angular separation between the isolated lepton and $\not\!\!E_T$ directions greater than 0.4. Events must contain at least one jet with $p_T > 20$ GeV after the calorimeter JES correction is applied, and $|\eta| < 2.5$. Upon application of all selection criteria, $N^e_{Wj} = 82747$ and $N^\mu_{Wj} = 57944$ W+jets candidates remain in the electron and muon channels, respectively.

Backgrounds originate from photons and jets that are misidentified as electrons and from $c\bar{c}$ and $b\bar{b}$ multi-jet events that produce an isolated muon. These multi-jet backgrounds are determined directly from the data using a "matrix method" consisting of the following steps: first, "loose" $W(\to \ell\nu)$+jets datasets are selected through application of all previously described selection criteria in each channel with the exception that the lepton isolation requirements are relaxed. This produces a set of loose candidate events, N^ℓ_L, in each lepton channel consisting of a mixture of real W+jets events, N^ℓ_W, and multi-jet background events, $N^\ell_{\rm MJ}$, with $N^\ell_L = N^\ell_W + N^\ell_{\rm MJ}$. Application of the stricter lepton isolation criteria used to extract the signal changes this mixture to $N^\ell_T = \epsilon^\ell_W N^\ell_W + \epsilon^\ell_{\rm MJ} N^\ell_{\rm MJ}$, where N^ℓ_T signifies the number of events in each channel satisfying the tighter isolation criteria and ϵ^ℓ_W and $\epsilon^\ell_{\rm MJ}$ denote the relative probabilities for loosely selected W boson and multi-jet events, respectively, to satisfy the stricter isolation criteria. A large sample of two-jet events is used to measure $\epsilon^e_{\rm MJ}$, and $\epsilon^\mu_{\rm MJ}$ is estimated from a similar two-jet dataset using a sample of back-to-back muon-plus-jet events with low $\not\!\!E_T$. The factors ϵ^ℓ_W are obtained from a large data sample of $Z \to \ell^+\ell^-$ events. Solving the equations for N^ℓ_W and $N^\ell_{\rm MJ}$ yields estimates for the fractional contributions of multi-jet background to the inclusive W+jets signal of $f^e_{\rm MJ} = (3.2 \pm 0.8)\%$ in the electron channel and $f^\mu_{\rm MJ} = (4.1 \pm 3.0)\%$ in the muon channel.

The channel $Z(\to \ell^+\ell^-)$+jets contributes as background when one of the leptons from the Z boson decay fails to be reconstructed. An estimate of this background follows from MC simulations of Z+jets production produced with ALPGEN v2.05 [17] using the CTEQ6L [18] PDF set, the PYTHIA v6.323 [19] generator for the parton fragmentation and hadronization, the MLM prescription [20] to avoid an over-counting of final state jets, and EVTGEN [21] to decay the heavy hadrons. A GEANT [22] based program simulates the effects of detector response, and the same reconstruction software is employed as used for data. This procedure results in estimates for the fractional contaminations of $f_Z^e = (0.9 \pm 0.1)\%$ for $Z(\to e^+e^-)$+jets and $f_Z^\mu = (5.0 \pm 0.7)\%$ for $Z(\to \mu^+\mu^-)$+jets. Quoted uncertainties derive mainly from systematic effects in the Z+jets ALPGEN cross section model that are estimated by varying the relative cross section of W+jets with respect to Z+jets by its uncertainties.

Extraction of samples of W+c-jet event candidates from the W+jets samples follows from selecting events with a μ-tagged jet. This jet must contain a reconstructed muon with $p_T > 4$ GeV and $|\eta| < 2.0$ that lies within a cone of $\Delta\mathcal{R}(\mu, \text{jet}) < 0.5$ with respect to the jet axis, and have JES corrected $p_T > 20$ GeV before including the muon and neutrino energies. The muon must be detected in both of the outer two layers of the muon spectrometer, and its muon spectrometer track must be matched to a reconstructed track in the central tracker. Background suppression of $Z(\to \mu^+\mu^-)$+jets events entails rejecting events in which the dimuon invariant mass exceeds 70 GeV in the muon channel without restricting the charges of the muons. Application of all selection criteria yields N_{OS}^e and N_{SS}^e events in the electron channel, and N_{OS}^μ and N_{SS}^μ events in the muon channel as reported in Table I. Estimated multi-jet backgrounds in the μ-tagged jet data samples determined following the matrix method are $N_{\text{OS}}^{e,\text{MJ}}$ and $N_{\text{SS}}^{e,\text{MJ}}$ events in the electron channel, and $N_{\text{OS}}^{\mu,\text{MJ}}$ and $N_{\text{SS}}^{\mu,\text{MJ}}$ events in the muon channel as listed in Table I. Estimates of the WW, $t\bar{t}$ and single top backgrounds from MC are denoted $N_{\text{OS}}^{e,WW}$, $N_{\text{SS}}^{e,WW}$, $N_{\text{OS}}^{e,t\bar{t}}$, $N_{\text{SS}}^{e,t\bar{t}}$, $N_{\text{OS}}^{e,t\bar{b}}$ and $N_{\text{SS}}^{e,t\bar{b}}$ events, respectively, in the electron channel, and $N_{\text{OS}}^{\mu,WW}$, $N_{\text{SS}}^{\mu,WW}$, $N_{\text{OS}}^{\mu,t\bar{t}}$, $N_{\text{SS}}^{\mu,t\bar{t}}$, $N_{\text{OS}}^{\mu,t\bar{b}}$ and $N_{\text{SS}}^{\mu,t\bar{b}}$ events, respectively, in the muon channel as given in Table I. The estimate of the single top background follows from the $t\bar{b}$ and $t\bar{b}q$ events produced with the COMPHEP [23] generator followed by full detector simulation. The quoted uncertainties on the WW, $t\bar{t}$ and single top background predictions given in Table I are dominated by the uncertainties in their cross section measurements [24, 25, 26]. Lepton charges are well measured at D0, and uncertainties from charge mis-identification are very small.

The acceptance times efficiencies, ϵ_c^ℓ $(\ell = e, \mu)$, of the W+c-jet selections relative to inclusive W+jets in each W boson decay channel is estimated from the MC simulation, and includes MC to data correction factors estimated using independent data calibration samples. The absolute efficiency of reconstructing a W boson with at least one jet cancels in the ratio. The relative acceptance includes effects of charm quark to hadron fragmentation, charmed hadron semi-muonic decay and the residual missing calorimeter energy from the muon and neutrino in the μ-tagged jet. The relative efficiency accounts for muon identification and track reconstruction effects. Charm quark fragmentation and charm hadron decay uncertainties are constrained by previous experiments [27, 28] and contribute 4.5% and 9.5%, respectively, to the acceptance uncertainties in both channels. The correction included in the acceptance for the missing contribution to the jet p_T from the muon and neutrino energies adjusts the jet p_T spectrum of W+c-jet candidate events appropriately to the particle level, as verified by a MC closure test. A large sample of $J/\psi \to \mu^+\mu^-$ events collected at D0 is employed to correct the jet-muon reconstruction efficiency, $(58.7 \pm 2.8)\%$, computed from the MC simulation, by a factor of 0.89 ± 0.06. This correction is found to be independent of the jet p_T. The final acceptance times efficiencies are found to be $\epsilon_c^e = (1.24 \pm 0.22)\%$ and $\epsilon_c^\mu = (1.22 \pm 0.23)\%$.

The presence of two muons in the muon channel increases the trigger selection efficiency of the W+c-jet candidates compared to the inclusive W+jets data sample. The divisor factor $K_T^\mu = 1.18 \pm 0.12$, extracted from the probability of events being selected when only the jet-muon fires the trigger, corrects for the bias in W+c-jet selection in the muon channel. In the electron channel the factor K_T^e is unity as the trigger efficiency cancels in the ratio.

The W+c-jet cross section ratio is extracted using

$$\frac{\sigma\left[W(\to \ell\nu) + c\text{-jet}\right]}{\sigma\left[W(\to \ell\nu) + \text{jets}\right]} = \frac{\frac{1}{\epsilon_c^\ell K_T^\ell}\left[N_{\text{OS}}^\ell - f_c^\ell\left(N_{\text{SS}}^\ell - N_{\text{SS}}^{\ell,\text{MJ}} - N_{\text{SS}}^{\ell,WW} - N_{\text{SS}}^{\ell,t\bar{t}} - N_{\text{SS}}^{\ell,t\bar{b}}\right) - N_{\text{OS}}^{\ell,\text{MJ}} - N_{\text{OS}}^{\ell,WW} - N_{\text{OS}}^{\ell,t\bar{t}} - N_{\text{OS}}^{\ell,t\bar{b}}\right]}{(1 - f_Z^\ell - f_{\text{MJ}}^\ell)N_{Wj}^\ell},$$

which requires one further correction in each channel, f_c^ℓ, for the small correlation between the jet-muon and W boson charges that arises in W+light-quark jet events. The factor f_c^ℓ is determined from fully simulated W+jet events as the ratio of the predicted number of OS μ-tagged jets to SS μ-tagged jets in all background samples that pass the same selection criteria as defined for the data sample. Processes considered include W+u,d,s, W+g, W+$c\bar{c}$, W+$b\bar{b}$, and W+c-jet, where the c quark does not decay semi-muonically in the last case. The f_c^ℓ

TABLE I: Summary of quantities to estimate the W+c-jet cross section ratio. The first uncertainties quoted are statistical and the second systematic.

jet p_T [GeV]	(20–30)	(30–45)	(45–200)	(20–200)
		$W \to e\nu$ decay channel		
N^e_{Wj}	35695	24412	22640	82747
N^e_{OS}	83	77	85	245
N^e_{SS}	45	41	68	154
$N^{e,\mathrm{MJ}}_{\mathrm{OS}}$	4.5±1.0±1.2	4.2±0.9±1.1	4.6±1.0±1.2	13.3±2.6±3.4
$N^{e,\mathrm{MJ}}_{\mathrm{SS}}$	5.6±1.1±1.4	5.1±1.0±1.3	8.5±1.5±2.2	19.3±2.9±4.9
$N^{e,WW}_{\mathrm{OS}}$	1.8±0.6	2.1±0.7	2.3±0.8	6.2±2.1
$N^{e,WW}_{\mathrm{SS}}$	0.4±0.1	0.6±0.2	0.9±0.3	1.9±0.5
$N^{e,t\bar{t}}_{\mathrm{OS}}$	2.4±0.6	4.6±1.1	11.8±2.8	18.8±4.5
$N^{e,t\bar{t}}_{\mathrm{SS}}$	2.1±0.5	4.1±1.0	10.0±2.4	16.1±3.9
$N^{e,t\bar{b}}_{\mathrm{OS}}$	1.1±0.3	2.1±0.6	3.1±0.9	6.3±1.8
$N^{e,t\bar{b}}_{\mathrm{SS}}$	0.8±0.2	1.4±0.4	2.5±0.7	4.6±1.3
f^e_c	1.183±0.017±0.018	1.164±0.019±0.017	1.118±0.024±0.017	1.149±0.007±0.017
ϵ^e_c	$0.0113\pm0.0015^{+0.0017}_{-0.0017}$	$0.0125\pm0.0011^{+0.0019}_{-0.0019}$	$0.0125\pm0.0020^{+0.0019}_{-0.0019}$	$0.0124\pm0.0012^{+0.0019}_{-0.0019}$
$\frac{\sigma[W(\to e\nu)+c\text{-jet}]}{\sigma[W(\to e\nu)+\text{jets}]}$	$0.079\pm0.031^{+0.013}_{-0.022}$	$0.100\pm0.038^{+0.017}_{-0.016}$	$0.043\pm0.049^{+0.007}_{-0.007}$	$0.073\pm0.023^{+0.012}_{-0.014}$
		$W \to \mu\nu$ decay channel		
N^μ_{Wj}	27378	17325	13241	57944
N^μ_{OS}	76	64	63	203
N^μ_{SS}	28	38	56	122
$N^{\mu,\mathrm{MJ}}_{\mathrm{OS}}$	4.6±1.8±3.3	3.8±1.5±2.7	3.8±1.5±2.7	12.2±4.6±8.7
$N^{\mu,\mathrm{MJ}}_{\mathrm{SS}}$	2.0±1.3±1.4	2.8±1.7±2.0	4.1±2.5±2.9	8.8±5.4±6.3
$N^{\mu,WW}_{\mathrm{OS}}$	0.8±0.3	1.6±0.5	1.8±0.6	4.2±1.6
$N^{\mu,WW}_{\mathrm{SS}}$	0.3±0.1	0.3±0.1	0.6±0.2	1.2±0.4
$N^{\mu,t\bar{t}}_{\mathrm{OS}}$	1.2±0.3	2.3±0.6	5.8±1.4	9.3±2.2
$N^{\mu,t\bar{t}}_{\mathrm{SS}}$	1.0±0.2	2.0±0.5	5.1±1.2	8.1±1.9
$N^{\mu,t\bar{b}}_{\mathrm{OS}}$	0.7±0.2	1.4±0.4	2.1±0.6	4.2±1.2
$N^{\mu,t\bar{b}}_{\mathrm{SS}}$	0.5±0.1	0.8±0.1	1.8±0.5	3.1±0.9
f^μ_c	1.195±0.025±0.014	1.174±0.027±0.013	1.121±0.035±0.013	1.148±0.007±0.013
ϵ^μ_c	$0.0110\pm0.0011^{+0.0016}_{-0.0017}$	$0.0122\pm0.0013^{+0.0018}_{-0.0019}$	$0.0148\pm0.0018^{+0.0022}_{-0.0023}$	$0.0122\pm0.0012^{+0.0018}_{-0.0019}$
K^μ_T	1.18±0.02±0.12	1.18±0.02±0.12	1.18±0.02±0.12	1.18±0.02±0.12
$\frac{\sigma[W(\to \mu\nu)+c\text{-jet}]}{\sigma[W(\to \mu\nu)+\text{jets}]}$	$0.123\pm0.037^{+0.024}_{-0.033}$	$0.076\pm0.050^{+0.016}_{-0.013}$	$0.000\pm0.058^{+0.014}_{-0.008}$	$0.075\pm0.031^{+0.015}_{-0.017}$
		Combined $W \to e\nu$ and $W \to \mu\nu$ decay channels		
$\frac{\sigma[W(\to \ell\nu)+c\text{-jet}]}{\sigma[W(\to \ell\nu)+\text{jets}]}$	$0.097\pm0.024^{+0.016}_{-0.026}$	$0.091\pm0.031^{+0.016}_{-0.015}$	$0.025\pm0.038^{+0.005}_{-0.004}$	$0.074\pm0.019^{+0.012}_{-0.014}$

are parameterized in terms of jet p_T as $f_c^\ell = a_\ell + b_\ell \times p_T$, with $a_e = 1.223 \pm 0.016$, $a_\mu = 1.241 \pm 0.023$, $b_e = -0.0017 \pm 0.0003$, and $b_\mu = -0.0019 \pm 0.0004$, where all quoted uncertainties of the parameters are statistical; f_c^ℓ decreases with increasing jet p_T because the sub-process $q\bar{q} \to Wg$ dominates $qg \to Wq'$ at high jet p_T. Systematic uncertainties in f_c^ℓ arise mainly from the cross section and jet fragmentation models. The f_c^ℓ are nearly independent of the absolute charged multiplicity per jet and the W+light-jets cross section. This has been verified by comparing the ratio of all OS tracks to all SS tracks found in jets in the inclusive W+jets data sample. The f_c^ℓ depend instead on the $K^\pm/\pi^\pm$ ratio per jet and the relative cross section for W boson plus heavy quark jet final states compared to W+light-jets. A 6% uncertainty is assigned to the weighted $\pi^\pm$ multiplicity based on a comparison of the difference between tracking efficiency in data and simulation, and a 20% uncertainty on the $K^\pm/\pi^\pm$ ratio is estimated based on comparing K_S^0 production in data to MC. Uncertainties in ALPGEN cross sections are estimated to be 50% for W+$b\bar{b}$, W+$c\bar{c}$, and W+c-jet, relative to W+light-jets [29]. A change of the W+c-jet cross section by ±100% does not lead to a significant effect in f_c^ℓ. The uncertainty due to PDFs on f_c^ℓ is estimated to be $^{+0.97}_{-0.64}$%. Overall systematic uncertainties are found to be 1.5% for f_c^e and 1.1% for f_c^μ, with the relative cross section contributions dominant. Adding a 0.6% uncertainty in each channel due to MC statistics yields $f_c^e = 1.149\pm0.018$ and $f_c^\mu = 1.148\pm0.015$ averaged over all $p_T > 20$ GeV.

Table I summarizes the cross section ratio measurements and their uncertainties for the electron and the muon channels for all jet $p_T > 20$ GeV and jet $|\eta| < 2.5$, and for three jet p_T bins with $|\eta| < 2.5$ in each bin. The ratio measurements benefit from cancellation of several uncertainties, notably the integrated luminosity [30], lep-

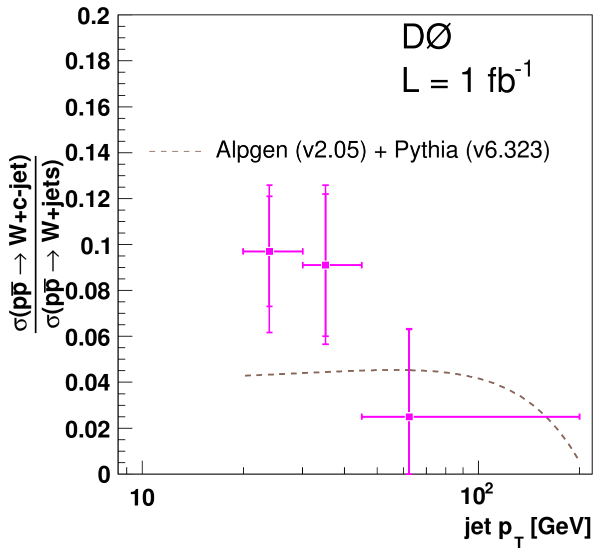

FIG. 1: Measured ratio $[\sigma(W{+}c\text{-jet})/\sigma(W{+}\text{jets})]$ for jet $p_T >$ 20 GeV and $|\eta| < 2.5$. The inner error bars around the data points show the statistical only uncertainties and the full bars represent the quadratic sum of statistical and systematic uncertainties. The systematic uncertainty on $W{+}c$-jet fraction includes the uncertainties due to JES, the jet p_T resolution, the background correction factor f_c^ℓ, and the product of the relative acceptance and efficiencies ϵ_c^ℓ. It also includes the uncertainty due to K_T^μ in the muon channel.

ton detection efficiency, and jet energy scale (JES). Table II lists remaining absolute systematic uncertainties on the measurement estimated from the MC simulation. These arise mainly from second order JES effects, jet p_T resolution (JPR), c-jet tagging efficiency, and the $W{+}c$-jet background correction factors f_c^ℓ.

The measured $W{+}c$-jet fractions integrated over $p_T >$ 20 GeV and $|\eta| < 2.5$ are

$$\frac{\sigma\,[W\,(\rightarrow e\nu) + c\text{-jet}]}{\sigma\,[W\,(\rightarrow e\nu) + \text{jets}]} \;=\; 0.073 \pm 0.023(\text{stat.})^{+0.012}_{-0.014}(\text{syst.}),$$
$$\frac{\sigma\,[W\,(\rightarrow \mu\nu) + c\text{-jet}]}{\sigma\,[W\,(\rightarrow \mu\nu) + \text{jets}]} \;=\; 0.075 \pm 0.031(\text{stat.})^{+0.015}_{-0.017}(\text{syst.}).$$

Since the $W \rightarrow e\nu$ and $W \rightarrow \mu\nu$ measurements are consistent with one another, and statistical uncertainties dominate, the two lepton channels are combined to yield

$$\frac{\sigma\,[W + c\text{-jet}]}{\sigma\,[W + \text{jets}]} = 0.074 \pm 0.019(\text{stat.})^{+0.012}_{-0.014}(\text{syst.}).$$

Systematic uncertainties are taken to be fully correlated in the two channels. This measurement can be compared to $W{+}c$-jet fraction predicted by ALPGEN and PYTHIA of 0.044±0.003, where the quoted theoretical uncertainty derives from the uncertainty on the CTEQ6.5 PDFs. Due

TABLE II: Fractional systematic uncertainties on the measurement in the $W \rightarrow e\nu$ and the $W \rightarrow \mu\nu$ channels.

	e channel				μ channel				
p_T	JES	JPR	f_c^e	ϵ_c^e	JES	JPR	f_c^μ	ϵ_c^μ	K_T^μ
GeV	%	%	%	%	%	%	%	%	%
20–30	$^{+0}_{-21.6}$	$^{+2.4}_{-4.8}$	$^{+3.8}_{-4.1}$	$^{+15.7}_{-15.6}$	$^{+0}_{-17.6}$	$^{+5.0}_{-7.5}$	$^{+2.5}_{-3.3}$	$^{+15.3}_{-16.2}$	±10
30–45	$^{+6.4}_{-4.3}$	$^{+2.1}_{-4.3}$	$^{+4.3}_{-4.7}$	$^{+14.5}_{-14.4}$	$^{+9.8}_{-0.7}$	$^{+4.5}_{-6.7}$	$^{+3.1}_{-4.3}$	$^{+14.1}_{-14.9}$	±10
45–200	$^{+2.2}_{-2.2}$	$^{+2.2}_{-4.5}$	$^{+6.9}_{-7.6}$	$^{+14.7}_{-14.6}$	$^{+27.7}_{-0}$	$^{+4.7}_{-7.0}$	$^{+4.0}_{-5.2}$	$^{+15.0}_{-15.8}$	±10
20–200	$^{+0}_{-9.0}$	$^{+2.3}_{-4.5}$	$^{+4.5}_{-5.2}$	$^{+15.1}_{-15.0}$	$^{+5.9}_{-2.4}$	$^{+4.7}_{-7.1}$	$^{+3.1}_{-4.3}$	$^{+14.9}_{-15.7}$	±10

to the relatively small contributions of $W{+}b\bar{b}$ and $W{+}c\bar{c}$ to inclusive $W{+}$jets, the model prediction of the $W{+}c$-jet rate has $\lesssim$ 5% sensitivity to their cross sections. Figure 1 shows the differential $W{+}c$-jet fraction, and compares the data to a model prediction using leading order QCD augmented by ALPGEN and PYTHIA.

As a test of the $W{+}c$-jet signal hypothesis, Fig. 2(a) compares data to ALPGEN and PYTHIA expectations in the background-subtracted distribution of the signed impact parameter significance, a/σ_a, for the jet-muon, where a is the projected distance of closest approach of the jet-muon to the event interaction point in the transverse plane, and σ_a is the estimated uncertainty on a. Data show satisfactory agreement with expectations for $W{+}c$-jet production and the underlying OS-SS ansatz after the subtraction of light and b quark jet contributions. Similarly, the distribution of the relative transverse momentum of the jet-muon with respect to the jet axis, p_T^{rel}, shows the consistency between data and the c-jet expectation as illustrated in Fig. 2(b).

To quantify the probability that the observed excess of OS events over SS events is due exclusively to background fluctuations, ensembles for OS, SS backgrounds and inclusive $W{+}$jets are generated that incorporate all the systematic uncertainties together with the correlations among the OS, SS backgrounds and $W{+}$jets expectations using Gaussian samplings of the uncertainties. The probability that background fluctuations could produce the observed fraction of the signal events in the inclusive $W{+}$jets sample is 2.5×10^{-4}, corresponding to a 3.5 σ significance for the $W{+}c$-jet hypothesis.

In conclusion, we have performed a measurement of the $W{+}c$-jet$/W{+}$jets cross section ratio at a hadron collider using both electron and muon decay channels of the W boson and utilizing the correlation between the charge of the jet-muon with that of the W boson. The probability that background fluctuations could produce an estimated $W{+}c$-jet fraction in $W{+}$jets equal to or larger than the one measured in data is 2.5×10^{-4}, which corresponds to a 3.5 σ significance of the observation. We find our measurement to be consistent with LO pertur-

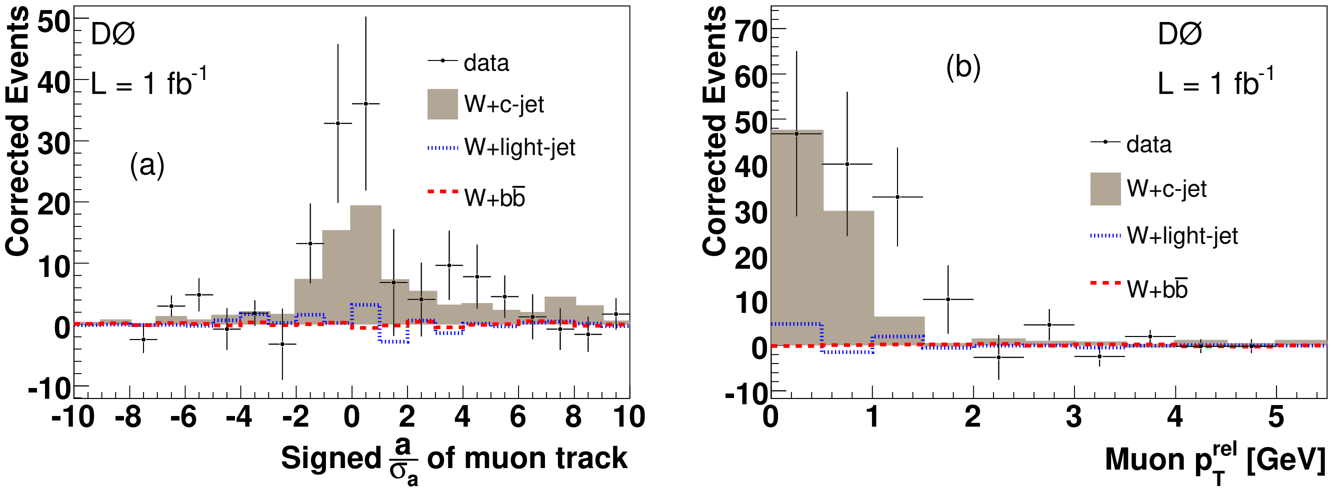

FIG. 2: Comparison of the background-subtracted ($N^\ell_{\rm OS} - f^\ell_c N^\ell_{\rm SS}$) data in the combined electron and muon channels with the simulation. (a) *Signed* significance in impact parameter of the jet-muon track with respect to the interaction point, (b) jet-muon transverse momentum relative to the jet axis ($p_T^{\rm rel}$).

bative QCD predictions of the W+c-jet production rate and with an s quark PDF evolved from Q^2 scales two orders of magnitude below those of this measurement. The measurement further provides direct experimental evidence of the underlying partonic process $qg \to Wq'$ that should dominate W boson production at the CERN Large Hadron Collider (LHC).

We thank the staffs at Fermilab and collaborating institutions, and acknowledge support from the DOE and NSF (USA); CEA and CNRS/IN2P3 (France); FASI, Rosatom and RFBR (Russia); CNPq, FAPERJ, FAPESP and FUNDUNESP (Brazil); DAE and DST (India); Colciencias (Colombia); CONACyT (Mexico); KRF and KOSEF (Korea); CONICET and UBACyT (Argentina); FOM (The Netherlands); STFC (United Kingdom); MSMT and GACR (Czech Republic); CRC Program, CFI, NSERC and WestGrid Project (Canada); BMBF and DFG (Germany); SFI (Ireland); The Swedish Research Council (Sweden); CAS and CNSF (China); and the Alexander von Humboldt Foundation.

---

[a] Visitor from Augustana College, Sioux Falls, SD, USA.
[b] Visitor from The University of Liverpool, Liverpool, UK.
[c] Visitor from ICN-UNAM, Mexico City, Mexico.
[d] Visitor from II. Physikalisches Institut, Georg-August-University, Göttingen, Germany.
[e] Visitor from Helsinki Institute of Physics, Helsinki, Finland.
[f] Visitor from Universität Zürich, Zürich, Switzerland.
[‡] Deceased.

[1] A. Abulencia *et al.* (CDF Collaboration), Phys. Rev. D **74**, 032008 (2006).
[2] V.M. Abazov *et al.* (D0 collaboration), Phys. Rev. Lett. **94**, 161801 (2005).
[3] T. Aaltonen *et al.* (CDF collaboration), Phys. Rev. Lett. **100**, 091803 (2008).
[4] U. Baur *et al.*, Phys. Lett. B **318**, 544 (1993).
[5] D.A. Mason *et al.* (NuTeV collaboration), Phys. Rev. Lett. **99**, 192001 (2007).
[6] M. Goncharov *et al.* (NuTeV collaboration), Phys. Rev. D **64**, 112006 (2001).
[7] S.A. Rabinowitz *et al.* (CCFR collaboration), Phys. Rev. Lett. **70**, 134 (1993).
[8] A.O. Bazarko *et al.* (CCFR collaboration), Z. Phys. **C65**, 189 (1995).
[9] P. Vilain *et al.* (Charm II Collaboration), Eur. Phys. J. **C11**, 19 (1999).
[10] H. Abramowicz *et al.* (CDHS collaboration), Z. Phys. **C15**, 19 (1982).
[11] M. Holder *et al.* (CDHS collaboration), Phys. Lett. B **69**, 377 (1977).
[12] H.L. Lai *et al.*, arXiv:hep-ph/0702268v2.
[13] G.C. Blazey *et al.*, in *Proceedings of the Workshop: QCD and Weak Boson Physics in Run II*, edited by U. Baur, R.K. Ellis, and D. Zeppenfeld, Fermilab-Pub-00/297 (2000).
[14] C. Butter *et al.*, arXiv:hep-ph/0803.0678v1 [hep-ph].
[15] K. Abe *et al.* (SLD Collaboration), Phys. Rev. Lett. **78**, 3442 (1997).
[16] V.M. Abazov *et al.* (D0 Collaboration), Nucl. Instrum. Methods Phys. Res. A **565**, 463 (2006).
[17] M.L. Mangano *et al.*, JHEP **0307**, 001 (2003). ALPGEN version 2.05 is used throughout.
[18] J. Pumplin *et al.*, JHEP **0207**, 012 (2002); D. Stump *et al.*, JHEP **0310**, 046 (2003).
[19] T. Sjöstrand *et al.*, Comput. Phys. Commun. **135**, 238 (2001). PYTHIA version 6.323 is used throughout.
[20] S. Hoeche *et al.*, arXiv:hep-ph/0602031v1.
[21] D.J. Lange, Nucl. Instrum. Methods Phys. Res. A **462**,

152 (2001).
[22] R. Brun and F. Carminati, CERN Program Library Long Writeup W5013 (1993).
[23] E. Boos *et al.* (CompHEP Collaboration), Nucl. Instrum. Methods Phys. Res. A **534**, 250 (2004).
[24] V.M. Abazov *et al.* (D0 Collaboration), Phys. Rev. Lett. **94**, 151801 (2005).
[25] V.M. Abazov *et al.* (D0 Collaboration), Phys. Rev. D **76**, 092007 (2007).
[26] V.M. Abazov *et al.* (D0 Collaboration), Phys. Rev. Lett. **98**, 181802 (2007).
[27] M. Artuso *et al.* (CLEO Collaboration), Phys. Rev. D **70**, 112001 (2004).
[28] W.-M. Yao *et al.* (Particle Data Group), J. Phys. G **33**, 1 (2006).
[29] V.M. Abazov *et al.* (D0 Collaboration), Phys. Rev. Lett. **98**, 181902 (2007).
[30] T. Andeen *et al.*, FERMILAB-TM-2365 (2007).